A Study of Partially Coherent Generalized Hermite Sinh-Gaussian Laser Beam Propagating in Various Biological Tissues

Faroq Saad[1]*, Halima Benzehoua[2], Omar Adil M. Ali[1], Abdelmajid Belafhal[2]
[1] Department of Radiological Imaging Technologies, Cihan University-Erbil, Erbil, Kurdistan Region, Iraq
[2] Laboratory LPNAMME, Laser Physics Group, Department of Physics, Faculty of Sciences,
Chouaïb Doukkali University, P. B 20, 24000 El Jadida, Morocco
* Corresponding authors E-mail: faroqsaad79@gmail.com,belafhal@gmail.com

***Abstract*—A new generalized laser beams named Generalized Hermite sinh- Gaussian with special profiles is introduced. Partially coherent Generalized Hermite sinh- Gaussian (PCGHshG) and their special profiles including partially coherent Hermite sinh-Gaussian (PCHshG) and partially coherent higher order sinh-Gaussian (PChoshG) beams traviling various tissues mediums are presented. Received field is obtained using extended Huygens-Fresnel method. Through numerical simulations, we examine how a partially coherent model, structural constant of biological tissue and parameters of beam affect the output average intensity. The obtained findings in this study can be beneficial in both medical topics diagnosis and imaging.**

***Index Terms*—: Partially coherent Generalized Hermite sinh-Gaussian beam; Huygens-Fresnel integral; Biological tissue.**

I. INTRODUCTION

Recently, researchers have conducted a detailed investigation of beam through a medium of soft tissue using model of power spectrum [1,2] and the extended Huygens-Fresnel method [3,4]. The interaction between light beams and biological tissue has captured significant attention through the last years to understand of developing the tissue imaging technology utlizing optical coherence tomography (OCT) method for disease diagnostics [5-7]. Investigations on the evolution properties of laser beam travel are tissue medium useful to improve both diagnostic and imaging quality [8]. In the literature, many studies have reported the investigation of different beam intensity patterns. Since then, the impact of coherence of partial on beam propagation in tissue medium is examined. The biological tissue structure has also been evaluated by determining the spreading beam and received Gaussian-Schell model distribution [9]. Lu et al. [10] have examined how biological tissue affects the also anomalous hollow beams. Additionally, intensity pattern of hollow Gaussian beam in tissue medium of biological has been discussed [11]. Similar observations are valid for partially coherent Lommel-Gaussian, rectangular multi-Gaussian beam model and coherent Laguerre-Gaussian and vortex beams have been presented, in same tissue medium [12-16]. In addition, further works have been done concerning index of scintillation and distribution of beam intensity in tissue mediums [17,18]. By observing the polarization profile and spatial characteristics of the scattered beams, the interaction of tissue-mimicking phantoms with light beams has been evaluated [19].

Moreover, Casperson and Tovar have introduced a set solution for the paraxial beam named Hermite-Sinusoidal-Gaussian (HSG), which describes a large variety of light beams propagating in complex optical systems [20,21]. The HSG beam allows describing a large family of light beams with structured intensity profiles [21,22]. In this regard, Bayraktar [23] has studied the received beam intensity for a partially coherent hyperbolic sinusoidal Gaussian in various tissue mediums. Additionally, generalized Hermite cosh-Gaussian beams as special cases for HSG beam are studied in various optical systems and media [24-32]. Spectral intensity of a pulsed chirped GHchG beam in tissue medium have been studied [33]. More recently, two further works have investigated the generalized Hermite cosh-Gaussian beam subject in upper dermis of human medium to discuss both intensity and pulsed chirped beam patterns [34-36]. Here, we present a new type of HSG beam as a generalized beam named Generalized Hermite sinh-Gaussian beam. It is of practical interest because its intensity distribution can be modified by selecting appropriate parameters of input beam.

Present paper aims to compare the average intensity of PHGHshG beam with two new types of their special cases including partially coherent Hermite sinh-Gaussian (PCHshG) beam and partially coherent higher order sinh-Gaussian (PChoshG) beam as they propagate in tissue medium of biological. The distinct parameters of the laser beams in these classes have garnered significant attention, making them suitable for practical applications. However, the evolution behavior of the PHGHshG beam in a biological tissue has not been studied. Our manuscript is structured as follows. Received intensity formula for a PHGHshG beam is obtained utlizing the integral of Huygens–Fresnel method, in Section 2. Many numerical simulations are given in comparing the characteristics for PHGHshG, PCHshG and PChshG beams in a biological tissue under different initial conditions, in Section 3. Finally, our results are concluded in Section 4.

II. PROPAGATION OF PCGHSHG BEAM THROUGH VARIOUS BIOLOGICAL TISSUES

The function of cross-spectral density (CSD) for partially

DOI: http://doi.org/10.24086/biohs2024/paper.1283

coherent PCGHshG beam in input plane described by.

$$W_0(\mathbf{r}_1,\mathbf{r}_2,z=0)=A_0^2\left(\frac{x_1}{\omega_0}\right)^l\left(\frac{x_2}{\omega_0}\right)^l\sinh^n(\Omega x_1)\sinh^n(\Omega x_2)\exp\left(-\frac{x_1^2+x_2^2}{\omega_0^2}\right)H_m\left(\frac{\sqrt{2}}{\omega_0}x_1\right)H_m\left(\frac{\sqrt{2}}{\omega_0}x_2\right)$$
$$\times\exp\left[-\frac{(x_1-x_2)^2}{2\sigma_0^2}\right]\left(\frac{y_1}{\omega_0}\right)^l\left(\frac{y_2}{\omega_0}\right)^l\sinh^n(\Omega y_1)\sinh^n(\Omega y_2)$$
$$\times\exp\left(-\frac{y_1^2+y_2^2}{\omega_0^2}\right)H_u\left(\frac{\sqrt{2}}{\omega_0}y_1\right)H_u\left(\frac{\sqrt{2}}{\omega_0}y_2\right)\exp\left[-\frac{(y_1-y_2)^2}{2\sigma_0^2}\right], \quad (1)$$

where the position vectors at the initial plane are r1=(x1, y1) and r2=(x2, y2), ω_0 refers to radius of waist, n represents beam order, l indicate hollowness parameter and Hj (.) denotes the jth order of the Hermite polynomials (j=m and u). A0 is amplitude of field, **Ω** represents the decentered parameters related to the $\sinh^n(t)$ and σ_0 is the coherence parameter.

The term $\sinh^n(t)$ can be expressed as [40].

$$\sinh^n(t)=\frac{1}{2^n}\sum_{s=0}^{n}\binom{n}{s}(-1)^n\exp(-a_{sn}t) \quad ,(2)$$

where $\binom{n}{s}$ indicates the binomial coefficient and $a_{sn}=2s-n$.

Fig. 1 schematizes the system that represents the behavior of light beam in a medium of biological tissue.

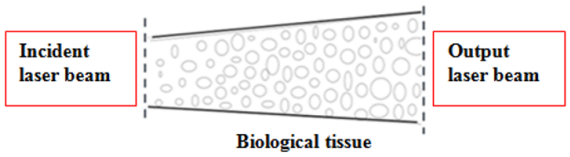

Figure 1: Laser beam traviling biological tissue.

Utilizing Huygens-Fresnel integral pricipale in calculating formula for a beam intensity propagating in medium of tissue as follows [38].

$$\langle I(\boldsymbol{\rho},z)\rangle=\frac{k^2}{4\pi^2z^2}\int_{-\infty}^{+\infty}\int_{-\infty}^{+\infty}\int_{-\infty}^{+\infty}\int_{-\infty}^{+\infty}W_0(\mathbf{r}_1,\mathbf{r}_2,z=0)$$
$$\times\exp\left\{-\frac{ik}{2z}\left[(x_1-\rho_x)^2+(y_1-\rho_y)^2-(x_2-\rho_x)^2-(y_2-\rho_y)^2\right]\right\}$$
$$\times\left\langle\exp\left[\psi(x_1,y_1,\rho_x,\rho_y)+\psi^*(x_2,y_2,\rho_x,\rho_y)\right]\right\rangle dx_1dx_2dy_1dy_2, \quad (3)$$

where $\boldsymbol{\rho}=(\rho_x,\rho_y)$ is position vector in output plane, z denotes distance of propagation, $\langle\ \rangle$ and * indicates the ensemble average and the complex conjugate, and $k=2\pi/\lambda$ refers to the wave number with λ is the wavelength of the beam.

ψ is solution of Rytov describing random part and phase perturbation for phase fluctuations induced by the turbulent biological tissue. The ensemble average term in Eq. (3), can be expressed as [38].

$$\left\langle\exp\left[\psi(x_1,y_1,\rho_x,\rho_y)+\psi^*(x_2,y_2,\rho_x,\rho_y)\right]\right\rangle=\exp\left\{-\left[\frac{(x_1-x_2)^2+(y_1-y_2)^2}{\rho_0^2}\right]\right\}, \quad (4)$$

The length of coherence ρ_0 for wave in biological tissue medium in [38] is given by,

$$|\rho_0|=0.22\left(C_n^2k^2z\right)^{-1/2}, \quad (5)$$

with C_n^2 indicates the refractive-index structure in tissue of biological and described by

$$C_n^2=\frac{\langle\delta n^2\rangle}{L_0^2(2-\varsigma)}, \quad (6)$$

where $\langle\delta n^2\rangle$ is the variance of refractive index, L_0 being the parameter of the outer scale related to the size of refractive index and ς is the parameter described of the tissue fractal dimension.

Substituting Eqs. (2) and (4) into Eq. (3), and using following formulae [37, 39].

$$\int_{-\infty}^{\infty}x^n e^{-px^2+2qx}H_m(ax)dx=\frac{1}{2^n}\sqrt{\frac{\pi}{p}}\exp\left(\frac{q^2}{p}\right)\sum_{k=0}^{[m/2]}\frac{(-1)^k m!}{k!(m-2k)!}\left(\frac{\alpha}{i\sqrt{p}}\right)^{m+n-2k}H_{m+n-2k}\left(\frac{iq}{\sqrt{p}}\right), \quad with\ \mathrm{Re}(p)>0 \quad (7)$$

$$H_n(x+y)=\frac{1}{2^{n/2}}\sum_{k=0}^{n}\binom{n}{k}H_k\left(\sqrt{2}x\right)H_{n-k}\left(\sqrt{2}y\right), \quad (8)$$

And

$$H_n(x)=\sum_{m=0}^{[n/2]}(-1)^m\frac{n!}{m!(n-2m)!}(2x)^{n-2m}, \quad (9)$$

After some processes calculations, intensity formula for PCGHshG in tissue medium is given by

$$\langle I(\boldsymbol{\rho},z)\rangle=\frac{A_0^2k^2}{4(\omega_0)^{4l}2^{4n+5l}z^2}\frac{1}{\sqrt{\beta_{1x}\beta_{2x}\beta_{1y}\beta_{2y}}}$$
$$\times\sum_{s_1=0}^{n}\sum_{s_2=0}^{n}\sum_{h_1=0}^{n}\sum_{h_2=0}^{n}\binom{n}{s_1}\binom{n}{s_2}\binom{n}{h_1}\binom{n}{h_2}\exp\left(\frac{(\gamma_{1x})^2}{\beta_{1x}}+\frac{(\gamma_{2x})^2}{\beta_{2x}}+\frac{(\gamma_{1y})^2}{\beta_{1y}}+\frac{(\gamma_{2y})^2}{\beta_{2y}}\right)$$
$$\times\sum_{k_1=0}^{[m/2]}\sum_{k_2=0}^{[m/2]}\frac{(-1)^{k_1+k_2}(m!)^2\left(2\sqrt{2}/\omega_0\right)^{m-2k_2}}{2^{(3m-2k_1-4k_2)/2}k_1!k_2!(m-2k_1)!(m-2k_2)!}\left(\frac{\sqrt{2}/\omega_0}{i\sqrt{\beta_{1x}}}\right)^{l+m-2k_1}\sum_{p=0}^{l+m-2k_1}\binom{l+m-2k_1}{p}H_p\left(\frac{\sqrt{2}i\gamma_{1x}}{\sqrt{\beta_{1x}}}\right)$$
$$\times\sum_{v=0}^{[l+m-2k_1-p/2]}\frac{(-1)^v(l+m-p-2k)!}{v!(l+m-2k_1-p-2v)!}\left(\frac{\sqrt{2}\alpha}{\sqrt{\beta_{1x}\beta_{2x}}}\right)^{2l+2m-2k_1-p-2k_2-2v}H_{2l+2m-2k_1-p-2k_2-2v}\left(\frac{i\gamma_{2x}}{\sqrt{\beta_{2x}}}\right)$$
$$\times\sum_{p_1=0}^{[u/2]}\sum_{p_2=0}^{[u/2]}\frac{(-1)^{p_1+p_2}(u!)^2\left(2\sqrt{2}/\omega_0\right)^{u-2p_2}}{2^{(3u-2p_1-4p_2)/2}p_1!p_2!(u-2p_1)!(u-2p_2)!}\left(\frac{\sqrt{2}/\omega_0}{i\sqrt{\beta_{1y}}}\right)^{l+u-2p_1}\sum_{t=0}^{l+u-2p_1}\binom{l+u-2p_1}{t}H_t\left(\frac{\sqrt{2}i\gamma_{1y}}{\sqrt{\beta_{1y}}}\right)$$
$$\times\sum_{g=0}^{[l+u-2p_1-t/2]}\frac{(-1)^g(l+u-t-2p_1)!}{g!(l+u-2p_1-t-2g)!}\left(\frac{\sqrt{2}\alpha}{\sqrt{\beta_{1y}\beta_{2y}}}\right)^{2l+2u-2p_1-t-2p_2-2g}H_{2l+2u-2p_1-t-2p_2-2g}\left(\frac{i\gamma_{2y}}{\sqrt{\beta_{2y}}}\right), \quad (10)$$

Where

$$\beta_{1x}=\frac{1}{\omega_0^2}+\frac{ik}{2z}+\frac{1}{2\sigma^2}+\frac{1}{\rho_0^2}, \quad (11a)$$

$$\beta_{1y}=\frac{1}{\omega_0^2}+\frac{ik}{2z}+\frac{1}{2\sigma^2}+\frac{1}{\rho_0^2}, \quad (11b)$$

$$\gamma_{1x}=\frac{ik\rho_x}{2z}-\frac{a_{s_1}\Omega}{2}, \quad (11c)$$

$$\gamma_{1y}=\frac{ik\rho_y}{2z}-\frac{a_{h_1}\Omega}{2}, \quad (11d)$$

$$\beta_{2x}=\frac{1}{\omega_0^2}-\frac{ik}{2z}+\frac{1}{\rho_0^2}-\frac{\alpha^2}{\beta_{1x}}, \quad (11e)$$

DOI: http://doi.org/10.24086/biohs2024/paper.1283

$$\beta_{2y} = \frac{1}{\omega_0^2} - \frac{ik}{2z} + \frac{1}{\rho_0^2} - \frac{\alpha^2}{\beta_{1y}}, \quad (11f)$$

$$\gamma_{2x} = \frac{\gamma_{1x}\alpha}{\beta_{1x}} - \frac{ik\rho_x}{2z} - \frac{a_{s_2}\Omega}{2}, \quad (11g)$$

And

$$\gamma_{2y} = \frac{\gamma_{1y}\alpha}{\beta_{1y}} - \frac{ik\rho_y}{2z} - \frac{a_{h_2}\Omega}{2}, \quad (11h)$$

With

$$\alpha = \frac{1}{2\sigma^2} + \frac{1}{\rho_0^2}. \quad (11i)$$

Eq. (10) is the main theoretical result that describes the behavior of PCGHshG beam in biological tissues. We will illustrate the numerical results of light beam distributions passing through biological tissues, in the coming Section.

III. RESULTS AND DISCUSSION

In this part, evolution properties of different partially coherent models including PCGHshG, PCHshG and PChoshG beams in different medium of biological tissues are simulated numerically. Parameters are chosen as: $A_0 = 1, \quad \lambda = 0.6238\mu m,$ $\sigma_0 = 2\mu m,$ $\omega_0 = 2\mu m,$ $n = 2,$ $l = 1,$ $m = 1,$ $u = 1$ and $\Omega = 0.1\mu m^{-1}$.

Figs. (2-4) investigates the (1D) and (3D) normalized average intensity to describe the influences of the spreading of the PHGHshG, PCHshG (Fig. 2), and PChoshG (Fig. 3) beams on different mediums of biological tissues, specifically the intestinal epithelium of a mouse, $C_n^2 = 0.06\times10^{-3}\,\mu m^{-1}$ (Fig. 2), deep dermis of a mouse $C_n^2 = 0.22\times10^{-3}\,\mu m^{-1}$ (Fig. 3), and upper dermis of a human $C_n^2 = 0.44\times10^{-3}\,\mu m^{-1}$ (Fig. 4), for various propagation distances. From the plots, it can be seen that the PHGHshG, the PCHshG and the PChoshG beams traveling various mediums of biological tissues can maintain almost its original intensity pattern in the initial plane (see the first column). The PHGHshG and the PCHshG profiles are four petal lobes structure with a dark central region. It is also observed a slight increase of the inter-lobes space for the PHGHshG compared to the PCHshG pattern. While the PChoshG beam is a solid pattern with the maximum central intensity. Upon propagation, PCGHshG and PCHsHG beams will change their original intensity pattern into flat-topped and Gaussian profiles, but the PChoshG beam can expand while still preserving their Gaussian-distribution profile for all tissues mediums.

On the other hand, the curves show that, as the C_n^2 increases, the average intensity distribution rises more quickly. For the PHGHshG and the PCHshG beams, the increase of parameter C_n^2 leads to the increase of the speed of the central peak. Additionally, for various biological tissues, PCHshG beam spreads fast during propagation and loses its original dark hollow center (or four-petal profile) more rapidly (see the second column) than in the PHGHshG pattern. This means that the PCGHshG beam demonstrates greater resistance against biological tissue turbulence.

Consequently, It can be seen that for both PHGHshG and PCHshG patterns, the speed of rise for the peak intensity center is slower with smaller C_n^2,this observation for smaller parameter C_n^2 can keep its dark center (or four-petal profile) better than the one with larger parameter C_n^2(upper dermis of a human).

It is evident that the considered beams can demonstrate a greater resistance against in turbulence of mouse tissue . One also can conclude that for the human upper dermis medium, the produced beam spread more rapidly compared to other mediums. Results also reveal that the beam quality depends on the biological tissue medium.

Effect of decentered parameter Ω on average intensity for three distributions including PCGHshG, PCHshG and PChoshG beams passing in two tissues mediums is illustrated in Figs. 5 and 6 at the near and far fields.

Iintensity shape at various biological tissues is significantly influenced by the beam parameter Ω. From plots, in the near field (z=2μm), one can observe the beams distributions propagating in both mediums of biological tissues, including the intestinal epithelium of a mouse (Fig. 5 a-b) and the upper dermis of a human (Fig. 6a-b), maintaining almost their original intensity patterns. Then, in the far-field, the beams with a small Ω configuration gradually lose their original central dark spot and transform in a Gaussian profile.

On other hand, beams with a large Ω configuration slowly lose their initial dark hollow center distribution during the transmission process and transform into a flat-topped distribution in the far field. It is also found from Figs. 5 and 6 that, the profiles in upper dermis of human will cause faster spreading than in the intestinal epithelium of mouse medium.

The coherence length σ0 effect on beam intensity for three distributions including PCGHshG, PCHshG and PCHhoshG beams in two types tissues is presented in Figs. 7 and 8, for near and far fields. For near distance (z=2μm) It can be seen from the plots that the considered beams with smaller σ0 spreads fast during propagation and lose its original central dark region more quickly (see the first row) compared to the one with large σ0 (see the second row). It is also found that, beams with all settings will transform into similar distribution of Gaussian beam in far plane.

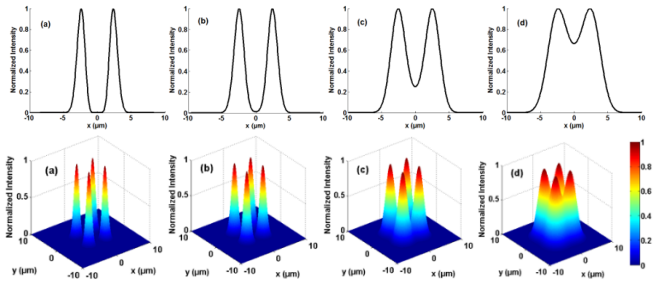

DOI: http://doi.org/10.24086/biohs2024/paper.1283

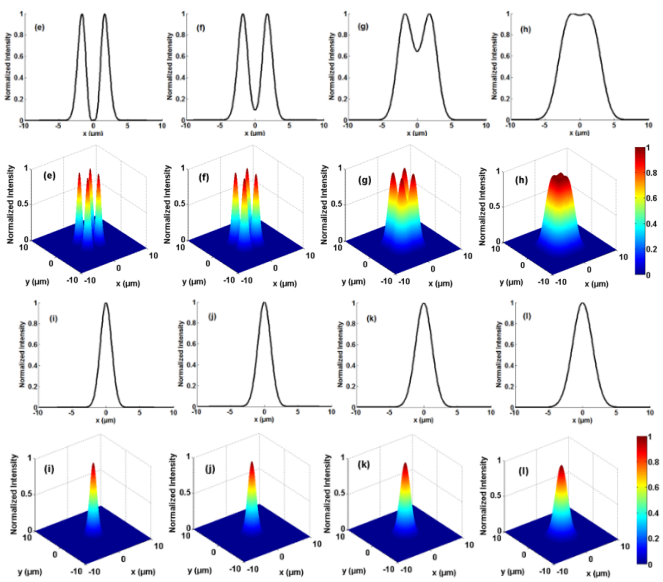

Figure 2: Normalized intensity for (a, b , c , d) PCGHshG (e, f, g, h) PCHshG
and (i, j, k l) PChoshG beams propagating in biological tissue for
at (a, e, i) z=0 (b, f, j) z=5μm (c, g, k) z=8μm and (d, h, l) z=10μm.

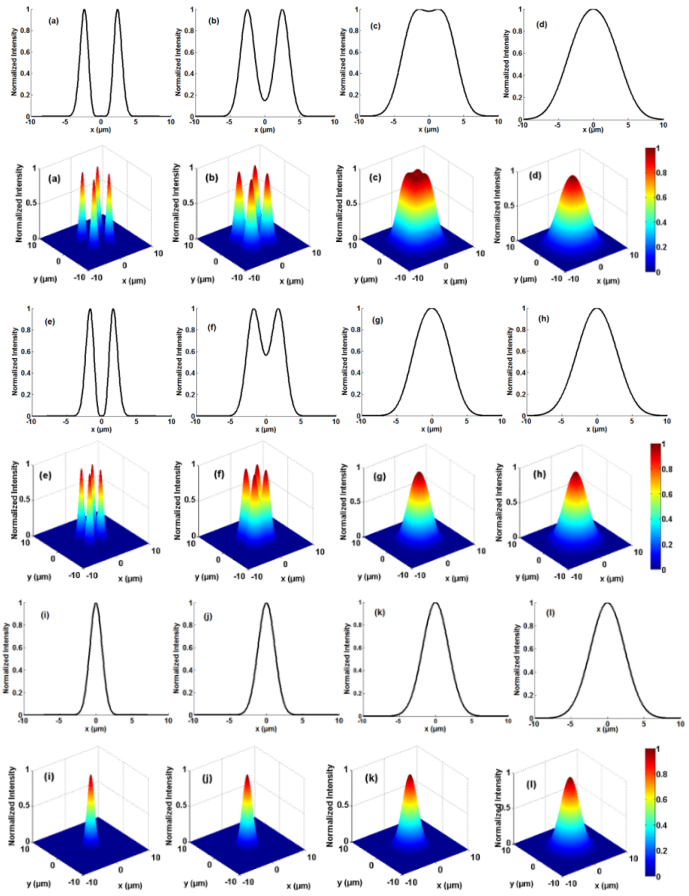

Figure 3: Normalized intensity for (a, b , c , d) PCGHshG (e, f, g, h) PCHshG
and (i, j, k l) PChoshG beams propagating in biological tissue for
at (a, e, i) z=0 (b, f, j) z=5μm (c, g, k) z=8μm and (d, h, l) z=10μm.

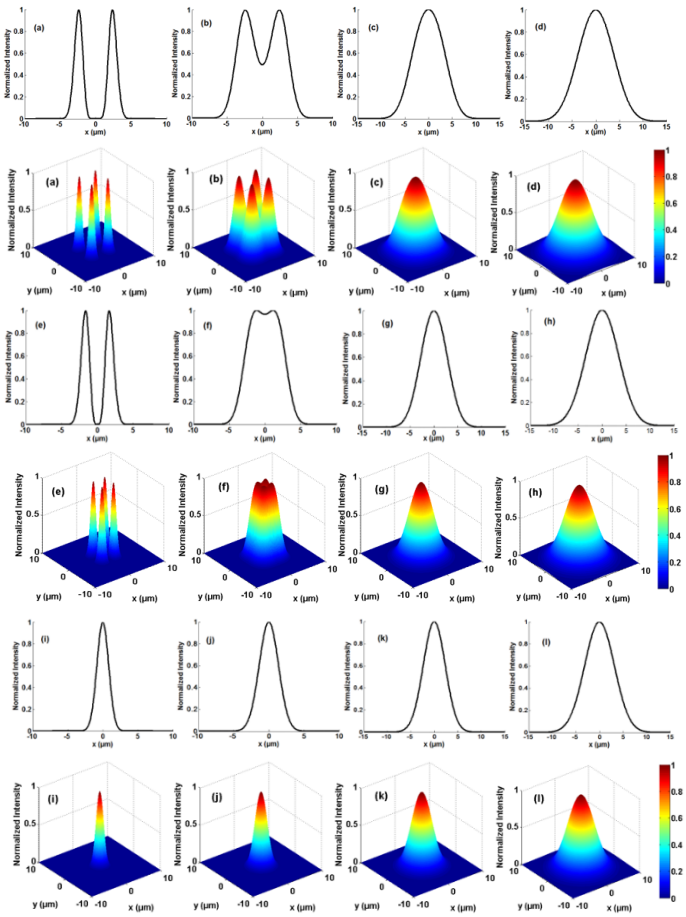

Figure 4: Normalized intensity for (a, b , c , d) PCGHshG (e, f, g, h) PCHshG
and (i, j, k l) PChoshG beams propagating in biological tissue for
at (a, e, i) z=0 (b, f, j) z=5μm (c, g, k) z=8μm and (d, h, l) z=10μm.

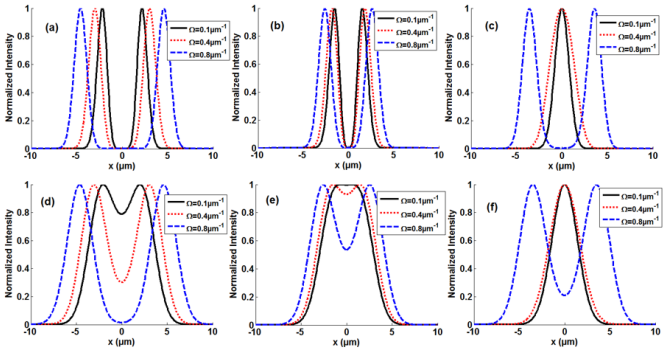

Figure 5: Normalized intensity of (a, d) PCGHshG (b, e) PCHshG and (c, f) PChoshG beams
in biological tissue for and various Ω
at (a, b, c) near-field (z=2μm) and (d, e, f) and far-field (z=10μm).

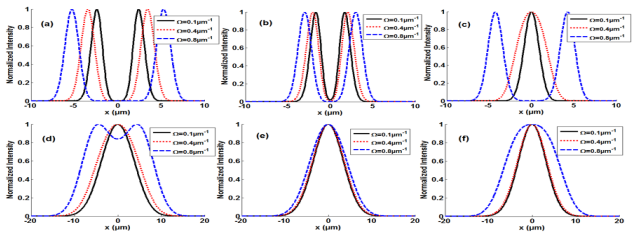

Figure 6: Normalized intensity of (a, d) PCGHshG (b, e) PCHshG and (c, f) PChoshG beams
in biological tissue for and various Ω
at (a, b, c) near-field (z=2μm) and (d, e, f) far-field (z=10μm).

DOI: http://doi.org/10.24086/biohs2024/paper.1283

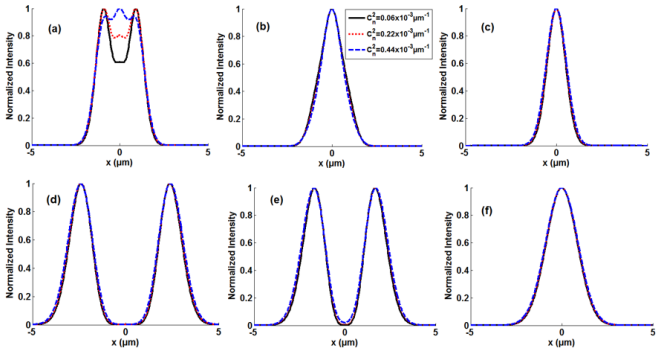

Figure 7: Normalized intensity of (a, d) PCGHshGB (b, e) PCHshGB and (c, f) PChshGB
propagating in biological tissues at near field z=2μm for two different spatial coherence length
(a, b, c) $\sigma_0 = 0.3\mu m$ and (d, e, f) $\sigma_0 = 2\mu m$.

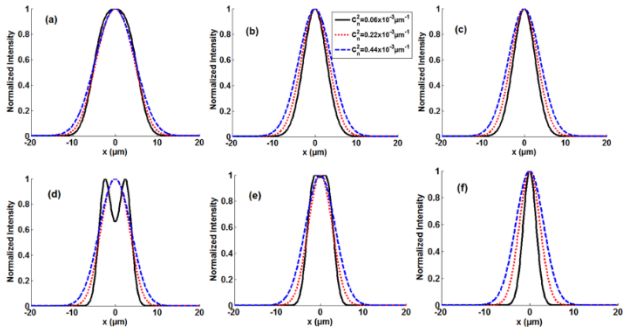

Figure 8: Normalized intensity of (a,d) PCGHshGB (b,e) PCHshGB and (c,f) PChshGB beams
propagating in biological tissues at far-field z=10μm
for two different spatial coherence length (a, b, c) $\sigma_0 = 0.3\mu m$ and (d, e, f) $\sigma_0 = 2\mu m$

One can note that PCHshG beam in the tissue medium exhibits similar propagation behavior to that of the PCGHshG beam, and it spreads faster than the latter distribution. The PCGHshG beam resists more against turbulence of biological tissues compares to the other beam distributions. One can also see from the plots that the increase of the parameter C_n^2 leads to the raise speed of the central peak profile rapidly.

CONCLUSION

In this paper, a novel light beam named Generalized hermite sinh-Gaussian has intoduced. An analytical formula of PCGHshG beam travileng various biological tissues mediums of is obtained utilizing Huygens-Fresnel integral. The behavior of PCGHshG beam and their special cases including PCHshG and PChoshG beams through various biological tissues are discussed. Intensity properties in biological tissues are illustrated. Our results show that evolution properties of the considered beams passing through in three tissues medium including, intestinal epithelium, deep dermis of mouse and upper dermis of human are determined by both parameters of initial beam and biological tissue system. Received intensity distribution is occurs faster in the medium of human upper dermis. Our findings can be beneficial in medical imaging and medical diagnosis.

REFERENCES

1. J.M. Schmitt, G. Kumar, Turbulent nature of refractive-index variations in biological tissue. Opt Lett 21, 1310–1312 (1996).
2. A.J. Radosevich, J. Yi, J.D. Rogers, V. Backman, Structural length-scale sensitivities of reflectance measurements in continuous random media under the Born approximation. Opt Lett 37, 5220–5222 (2012).
3. O. Korotkova, Random light beams: theory and applications. CRC Press, Boca Raton (2014).
4.] L. C. Andrews, R.L. Phillips, Laser beam propagation through random media. SPIE, Bellingham (2005).
5. D. Huang, E. A. Swanson, C. P. Lin, J. S. Schuman, W. G. Stinson, W. Chang, M. R. Hee, T. Flotte, K. Gregory, C. A. Puliafito, Optical coherence tomography, Science 254, 1178–1181 (1991).
6.] A. F. Ferchera, C. Hitzenbergera, G. Kampa, S. Y. El-Zaiat, Measurement of intraocular distances by backscattering spectral interferometry, Opt. Commun. 117, 43–48 (1995).
7. G. Husler, M. W. Lindner, Coherence radar and spectral radarnew tools for dermatological diagnosis, J. Biomed. Opt. 3, 21–31 (1998).
8. W. Gao, Change of coherence of light produced by tissue turbulence. J Quant Spectrosc Radiat Transfer 131, 52-8 (2013).
9. Wu Zhang Y., Wang Q., Hu Z.: Average intensity and spreading of partially coherent model beams propagating in a turbulent biological tissue. J Quant Spectrosc Radiat Transf 184, 308–15 (2016).
10. Y. Lu, X. Zhu, X., K. Wang, C. Zhao, Y. Cai,: Effects of biological tissues on the propagation properties of anomalous hollow beams. Optik 127, 1842-1847 (2016).
11. F. Saad, A. Belafhal, A theoretical investigation on the propagation properties of HollowGaussian beams passing through turbulent biological tissues. Optik 141, 72-82 (2017).
12. L.Yu, Y. Zhang, Beam spreading and wander of partially coherent Lommel-Gaussian beam in turbulent biological tissue. J. Quant. Spectrosc. Radiat. Transf. 217, 315-320 (2018).
13. D.J. Liu, H.Y. Zhong, H.M. Yin, A.Y. Dong, G.Q. Wang, Y.C. Wang, Spreading and coherence properties of a rectangular multi-Gaussian Schell-model beam propagating in biological tissues, Indian J. Phys. 95 571–577 (2020).
14. A. A. A. Ebrahim, A. Belafhal, Effect of the turbulent biological tissues on the propagation properties of Coherent Laguerre-Gaussian beams. Opt. Quant. Electron. 53, 179 196 (2021).
15. S. Chib, A. Belafhal, Analyzing the spreading properties of vortex beam in turbulent biological tissues. Opt. Quant. Electron. 55, 98-116 (2023).
16. D.J. Liu, H.Y. Zhong, H.M. Yin, A.Y. Dong, G.Q. Wang, Y.C. Wang, Spreading and coherence properties of a rectangular multi-Gaussian Schell-model beam propagating in biological tissues, Indian J. Phys. 95, 571–577 (2020).
17. H. Jin, W. Zheng, H.T. Ma, Y. Zhao, Average intensity and scintillation of light in a turbulent biological tissue, Optik 127, 9813–9820 (2016).
18. Y. Baykal, C. Arpali, S.A. Arpali, Scintillation index of optical spherical wave propagating through biological tissue, J. Mod. Opt. 64, 138–142 (2017).
19. A. Suprano, T. Giordani, I. Gianani, N. Spagnolo, K. Pinker, J. Kupferman, S. Arnon, U. Kleem, D. Gorpas, V. Ntziacgristos, F. Sciarrino, Propagation of structured light through tissue-mimicking phantoms, Opt. Express 28, 35427–35437 (2020).
20. L. W., Casperson, A. A. Tovar, Hermite-sinusoidal-Gaussian beams in complex optical systems. J. Opt. Soc. Am. A 15, 954–961 (1998).
21. L. W. Casperson, D. G. Hall, A. A. Tovar, Sinusoidal-Gaussian beams in complex optical systems. J. Opt. Soc. Am. A 14, 3341–3348 (1997).
22. A. A. Tovar, L. W., Casperson, Production and propagation of Hermite-sinusoidal-Gaussian laser beams. J. Opt. Soc. Am. A 15, 2425–2432 (1998).
23. M. Bayraktar, Propagation of partially coherent hyperbolic sinusoidal Gaussian beam in biological tissue. Optik 245, 167741-167748 (2021).
24. F. Saad, A. Belafhal, Investigation on propagation properties of a new optical vortex beam: generalized Hermite cosh-Gaussian beam. Opt. Quant. Electron. 55, 1-16 (2022).

DOI: http://doi.org/10.24086/biohs2024/paper.1283

25. F. Saad, A. Belafhal, A comprehensive investigation on the propagation properties of a Generalized Hermite Cosh-Gaussian beam through atmospheric turbulence. Opt. Quant. Electron. 55, 1037-1048 (2023).
26. F. Saad, A. Belafhal: A detailed investigation of a Generalized Hermite cosh-Gaussian beam propagating in uniaxial crystals orthogonal to the optical axis. Opt. Quant. Electron. 55, 1080-1091 (2023).
27. F. Saad, H. Benzehoua, A. Belafhal, Oceanic turbulent effect on the received intensity of a generalized Hermite cosh-Gaussian beam. Opt. Quant. Electron. 56, 1-15 (2023).
28. F. Saad, H. Benzehoua, A. Belafhal, Propagation behavior of a generalized Hermite cosh-Gaussian laser beam through marine environment. Opt. Quant. Electron. 56, 1-12 (2023).
29. H. Benzehoua, F. Saad, A. Belafhal, A theoretical study of spectral properties of generalized chirped Hermite cosh Gaussian pulse beams in oceanic turbulence. Opt. Quant. Electron. 55, 1-14 (2023).
30. Saad, F.: Propagation properties of general model vortex higher-order Cosh-Gaussian laser beam through uniaxial crystal orthogonal to the optical axis. Opt. Quant. Electron. 56, 790 (1-15) (2024).
31. Saad, F., Benzehoua, H., Belafhal, A.: Evolution properties of Laguerre higher order cosh Gaussian beam propagating through fractional Fourier transform optical system. Opt. Quant. Electron. 56, 1-15 (2024).
32. Saad, F., Hricha, Z., Belafhal, A.: Propagation properties of higher-order cosine-hyperbolic-Gaussian beams in a chiral medium. Opt. Quant. Electron. 56, 1-15 (2024).
33. H. Benzehoua, F. Saad, A. Belafhal, Spectrum changes of pulsed chirped Generalized Hermite cosh-Gaussian beam through turbulent biological tissues. Optik 294, 1-10 (2023).
34. F. Saad, H. Benzehoua, A. Belafhal, Analysis on the propagation characteristics of a Generalized Hermite cosh-Gaussian beam through human upper dermis tissue. Opt. Quant. Electron. Vol. 56, 1-15 (2024).
35. Benzehoua, H., Saad, F., Bayraktar, M., Chatzinotas, S., Belafhal, A. :Impact of human upper dermis tissue on the spectral intensity of a pulsed chirped general model vortex higher-order cosh-Gaussian beam. Opt. Quant. Electron. 56, 850 (1-16) (2024).
36. Benzehoua, H., Saad, F., Bayraktar, M., Chatzinotas, S., Belafhal, A. : Analyzing the theoretical evolution behavior of Laguerre higher-order cosh-Gaussian beam propagating through liver tissue. Opt. Quant. Electron. 56, 767(1-14) (2024).
37. M. Abramowitz, I. Stegun, Handbook of Mathematical Functions with Formulas, Graphs, and Mathematical Tables, U. S., Department of Commerce (1970).
38. L. C. Andrews, R. L. Philips, Laser beam propagation through Random media. SPIE Press, Washington (1998).
39. A. Belafhal, Z. Hricha, L. Dalil-Essakali, T. Usman, A note on some integrals involving Hermite polynomials encountered in caustic optics. Adv. Math. Models Appl. 5, 313–319 (2020).
40. I.S. Gradshteyn, I. M. Ryzhik, Tables of Integrals, Series, and Product, 5th edn. Academic Press, New York (1994).

DOI: http://doi.org/10.24086/biohs2024/paper.1283